Functional interaction with filamin A and intracellular Ca^{2+} enhance the surface membrane expression of a small-conductance Ca^{2+}-activated K^+ (SK2) channel

Sassan Rafizadeh[a,1], Zheng Zhang[a,1], Ryan L. Woltz[a], Hyo Jeong Kim[b], Richard E. Myers[a], Ling Lu[a,c], Dipika Tuteja[a], Anil Singapuri[a], Amir Ali Ziaei Bigdeli[a], Sana Ben Harchache[a], Anne A. Knowlton[a,d], Vladimir Yarov-Yarovoy[e], Ebenezer N. Yamoah[b], and Nipavan Chiamvimonvat[a,d,2]

[a]Division of Cardiovascular Medicine, [b]Center for Neuroscience, and [e]Department of Physiology and Membrane Biology, University of California, Davis, CA 95616; [c]Jiangsu Key Laboratory for Microbes and Functional Genomics, Jiangsu Engineering and Technology Research Center for Microbiology, College of Life Sciences, Nanjing Normal University, Nanjing 210046, China; and [d]Department of Veterans Affairs, Northern California Health Care System, Mather, CA 95655

Edited* by Richard W. Aldrich, University of Texas at Austin, Austin, TX, and approved May 30, 2014 (received for review December 18, 2013)

For an excitable cell to function properly, a precise number of ion channel proteins need to be trafficked to distinct locations on the cell surface membrane, through a network and anchoring activity of cytoskeletal proteins. Not surprisingly, mutations in anchoring proteins have profound effects on membrane excitability. Ca^{2+}-activated K^+ channels ($K_{Ca}2$ or SK) have been shown to play critical roles in shaping the cardiac atrial action potential profile. Here, we demonstrate that filamin A, a cytoskeletal protein, augments the trafficking of SK2 channels in cardiac myocytes. The trafficking of SK2 channel is Ca^{2+}-dependent. Further, the Ca^{2+} dependence relies on another channel-interacting protein, α-actinin2, revealing a tight, yet intriguing, assembly of cytoskeletal proteins that orchestrate membrane expression of SK2 channels in cardiac myocytes. We assert that changes in SK channel trafficking would significantly alter atrial action potential and consequently atrial excitability. Identification of therapeutic targets to manipulate the subcellular localization of SK channels is likely to be clinically efficacious. The findings here may transcend the area of SK2 channel studies and may have implications not only in cardiac myocytes but in other types of excitable cells.

ion channel trafficking | atrial myocytes | atrial fibrillation

Small-conductance Ca^{2+}-activated K^+ (SK or $K_{Ca}2$) channels are highly unique in that they are gated solely by changes in intracellular Ca^{2+} ($Ca^{2+}{}_i$) concentration. Hence, the channels function to integrate changes in Ca^{2+} concentration with changes in membrane potentials. SK channels have been shown to be expressed in a wide variety of cells (1–3) and mediate after-hyperpolarizations following action potentials in neurons (1, 4, 5). We have previously documented the expression of several isoforms of SK channels in human and mouse atrial myocytes that mediate the repolarization phase of the atrial action potentials (6, 7). We further demonstrated that SK2 ($K_{Ca}2.2$) channel knockout mice are prone to the development of atrial arrhythmias and atrial fibrillation (AF) (8). Conversely, a recent study by Diness et al. suggests that inhibition of SK channels may prevent AF (9). Together, these studies underpin the importance of the precise control for the expression of these ion channels in atria and their potential to serve as a future therapeutic target for AF.

Current antiarrhythmic agents target the permeation and gating properties of ion channel proteins; however, increasing evidence suggests that membrane localization of ion channels may also be pharmacologically altered (10). Furthermore, a number of disorders have been associated with mistrafficking of ion channel proteins (11, 12). We have previously demonstrated the critical role of α-actinin2, a cytoskeletal protein, in the surface membrane localization of cardiac SK2 channels (13, 14). Specifically, we demonstrated that cardiac SK2 channel interacts with α-actinin2 cytoskeletal protein via the EF hand motifs in α-actinin2 protein and the helical core region of the calmodulin (CaM) binding domain (CaMBD) in the C terminus of SK2 channel. Moreover, direct interactions between SK2 channel and α-actinin2 are required for the increase in cell surface localization of SK2 channel.

Here, to further define the functional interactome of SK2 channel in the heart, we demonstrate the role of filamin A (FLNA), another cytoskeletal protein, in SK2 channel surface membrane localization. In contrast to α-actinin2 protein, FLNA interacts not with the C terminus, but with the N terminus of the cardiac SK2 channel. FLNA is a scaffolding cytoskeletal protein with two calponin homology domains that has been shown to be critical for the trafficking of a number of membrane proteins (15–19). Our data demonstrate that FLNA functions to enhance membrane localization of SK2 channels. Moreover, using live-cell imaging, we demonstrate the critical roles of $Ca^{2+}{}_i$ on the membrane localization of SK2 channel when the channels are coexpressed with α-actinin2, but not FLNA. A decrease in $Ca^{2+}{}_i$ results in a significant decrease in SK2 channel membrane localization. Our findings may have important clinical implications. A rise in $Ca^{2+}{}_i$—for example, during rapid pacing or atrial tachyarrhythmias—is predicted to increase the membrane localization of SK2 channel and result in the abbreviation of the atrial action potentials and maintenance of the arrhythmias.

Significance

The precise subcellular localization of ion channel proteins is necessary for the proper function of excitable cells. The trafficking of several ion channels is dependent on the interaction of the ion channel proteins with cytoskeletal proteins, underpinned by a number of diseases in which the defect lies with the interacting proteins. Here, we demonstrate the role of filamin A, a cytoskeletal protein, in augmenting the membrane expression of small-conductance, Ca^{2+}-activated K^+ channels ($K_{Ca}2.2$ or SK2) in atrial myocytes. We further demonstrate that SK2 channel trafficking is Ca^{2+}-dependent in the presence of another cytoskeletal protein, α-actinin2, thereby establishing the role of filamin A, α-actinin2, and intracellular Ca^{2+} in trafficking of SK2 channels. The findings may have implications in other excitable cells.

Author contributions: S.R., Z.Z., R.L.W., R.E.M., L.L., V.Y.-Y., E.N.Y., and N.C. designed research; S.R., Z.Z., R.L.W., H.J.K., R.E.M., L.L., D.T., A.S., A.A.Z.B., S.B.H., and V.Y.-Y. performed research; A.A.K., E.N.Y., and N.C. contributed new reagents/analytic tools; S.R., Z.Z., R.L.W., V.Y.-Y., and N.C. analyzed data; and S.R., Z.Z., R.L.W., V.Y.-Y., E.N.Y., and N.C. wrote the paper.

The authors declare no conflict of interest.

*This Direct Submission article had a prearranged editor.

[1]S.R. and Z.Z. contributed equally to this work.

[2]To whom correspondence should be addressed. E-mail: nchiamvimonvat@ucdavis.edu.

This article contains supporting information online at www.pnas.org/lookup/suppl/doi:10.1073/pnas.1323541111/-/DCSupplemental.

Results

C Terminus of FLNA Interacts with the N Terminus of SK2. We have previously demonstrated that the C terminus of human cardiac SK2 channel interacts with a cytoskeletal protein, α-actinin2. Moreover, the protein–protein interaction between SK2 and α-actinin2 results in an increase in the surface membrane expression SK2 channels (13, 14). To determine possible interacting proteins with the N terminus of human cardiac SK2 channel, we screened the human heart library (Clontech; catalog no. HL4042AH) using the intracellular N-terminal fragment of SK2 channel (amino acids 1–145; termed SK2-N) in pGBKT7 vector, containing the binding domain (BD) as bait (Fig. 1*A*). One of the positive clones corresponded to the C-terminal 385 amino acids (2,262–2,647) of FLNA in pACT2 vector, containing the activating domain (termed FLNA-C; Fig. 1*B*). We further confirmed the interaction between the N terminus of SK2 channel with FLNA-C using in vitro yeast two-hybrid assay. The interaction was confirmed three times, depicted as growth of colonies using high-stringency media (Fig. 1*C*). The inserts were also subcloned into reciprocal vectors and tested for interactions with similar results, indicating that the interactions were not vector-specific. Three different fragments of the C terminus of SK2 channel (SK2-C1, -C2, and -C3) served as negative controls and did not show interaction with FLNA-C (Fig. 1*C* and Fig. S1). Interactions between p53 and pGADT7-T served as a positive control (Fig. 1*C*).

Proline Residues in the PxxP Motif in the N Terminus of SK2 Channel Are Required for the Observed Interaction with FLNA. Data to support the specificity of the observed interactions between the N terminus of SK2 channel and the C terminus of FLNA were obtained by using a combination of site-directed mutagenesis and in vitro yeast two-hybrid assay to elucidate the sites necessary for the proposed interaction. Proline residues (P) in the consensus sequence of PxxP (where xx refers to any other amino acids) have been shown to be critical for the binding to FLNA proteins (16, 17). Closer inspection of the N terminus of SK2 channel revealed the PxxP motif with proline residues at positions 25 and 28 in the human cardiac SK2 channel. Double mutations of the proline residues to alanine (SK2-N P25,28A or SK2-N–MutI) abolished the in vitro interaction (Fig. 1*C*).

Ten single-point mutations of proline to alanine were then generated within the C terminus of FLNA (pACT2–FLNA-C; Fig. S1*A*). A mutation of proline at position 2,545 to alanine (FLNA-C P2545A) resulted in a decrease in the number of colonies under high-stringency conditions (Fig. S1*B*). Together, the data suggest that the proline residues within the PxxP motif in the N terminus of SK2 channel are necessary for the interactions with the specific proline residue within the C terminus of FLNA protein.

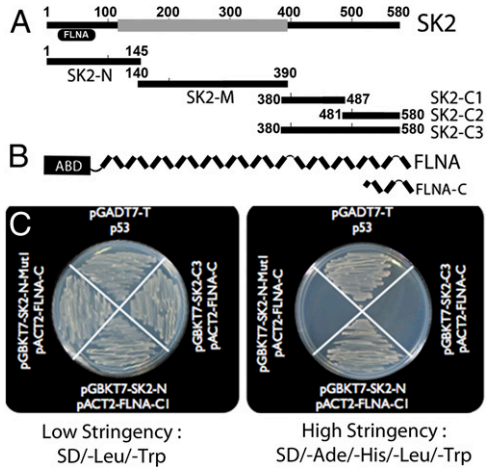

Fig. 1. The C terminus of FLNA directly interacts with the N terminus of SK2 channel. (*A*) Different regions of human cardiac SK2 channel in pGBKT7 vector were used as bait to screen the human heart library (Clontech). (*B*) By using the N terminus of human cardiac SK2 channel in pGBKT7 vector (pGBKT7–SK2-N) as bait to screen the human heart library, one clone corresponding to the C terminus of the FLNA protein in the prey vector (pACT2–FLNA-C) was identified as the putative interacting protein. (*C*) Interaction was confirmed three times by using the yeast two-hybrid assay depicted as growth of colonies in high-stringency media (SD/-Ade/-His/-Leu/-Trp). pGADT-7 with p53 served as a positive control. The C-terminal domain of SK2 channel in pGBKT7 (pGBKT7–SK2-C3) with FLNA-C served as a negative control. Closer inspection of the N terminus of SK2 channel revealed the PxxP motif with proline residues at positions 25 and 28 in the human cardiac SK2 channel. Double mutations of the proline residues to alanine (pGBKT7–SK2-N–MutI) abolished the in vitro interaction.

FLNA Colocalizes with SK2 Channel in Atrial Myocytes. To test the expression of FLNA in the heart, we performed immunofluorescence confocal laser scanning microscopic experiments using isolated mouse atrial myocytes. Single staining using anti-SK2 (Fig. 2 *A*, *a–c*) and anti-FLNA (Fig. 2 *A*, *d–f*) antibodies was performed (Fig. 2*A*). FLNA was found to be localized along the Z lines (Fig. S2*A*) and colocalized with SK2 channels by using double labeling (Fig. 2 *A*, *g–i* and *l*). A correlation coefficient of ∼0.8 was observed (Fig. 2*B*). Secondary antibodies only were used as negative controls (Fig. 2 *A*, *j* and *k*). The antibody specificity has been shown by our group for anti-SK2 (13, 14) and others for anti-FLNA antibodies (16–19). In addition, Western blot analyses were performed by using anti-FLNA antibody. A positive band at the expected size (∼280 kDa) was observed (Fig. 2*C*) using human left atrial (HLA) and mouse left atrial (MLA) and mouse right atrial (MRA) tissues.

FLNA Enhances Membrane Expression of SK2 Channels. To assess the functional role of the proposed interaction between FLNA and SK2 channel, both proteins were coexpressed in HEK 293 cells (Fig. S2*B*). Results were compared against cells expressing SK2 channel only. In cells transfected with SK2 channel only, the majority of the channel proteins showed intracellular localization, even though these cells show a small level of basal expression of FLNA (Fig. S2 *B*, *e–h*). In contrast, when FLNA was coexpressed, SK2 channels showed a localization pattern principally on the plasma membrane (Fig. S2 *B*, *i–l*). Repeat experiments were performed by using FLNA-deficient M2 cells, showing similar results as in HEK 293 cells (Fig. S2*C*).

Additionally, live-cell total internal reflection fluorescence microscopy (TIRF-M) using a human cardiac SK2 construct containing a C-terminal tdTomato fusion protein (Fig. 3*A*) was performed to further support the data from Fig. S2*B*. HEK 293 cells transfected with the vector containing tdTomato were used as a negative control showing a lack of fluorescence on the membrane in TIRF mode (Fig. 3 *B* and *C*). Coexpression of SK2 channel with FLNA significantly increased fluorescence intensity on the membrane (Fig. 3*E*) compared with expression of SK2 channel alone (Fig. 3*D*). Summary data are shown in Fig. 3*F*.

siRNA Knockdown of FLNA Reduces the Surface Membrane Expression of SK2 Channels in Neonatal Mouse Cardiomyocytes. To test the functional significance of FLNA on the surface membrane expression of SK2 channels in cardiac myocytes, siRNA-mediated knockdown of FLNA was performed in neonatal mouse cardiomyocytes (NMCMs) as shown in Fig. 4. We first assessed the efficiency and specificity of the siRNA knockdown of FLNA using quantitative RT-PCR and immunofluorescence confocal microscopy. Seventy-two hours after transfection yielded the highest knockdown efficiency at the protein level as assessed by using immunofluorescence confocal microscopy (Fig. 4*O*), whereas 48 h after transfection yielded a 60-fold decrease in FLNA mRNA (Fig. S2*D*). GAPDH was used as control (Fig. S2*D*). Previous studies using the same FLNA siRNA have yielded similar results (15). In control experiments using a nontargeting scramble siRNA, SK2 channel proteins were found to be localized

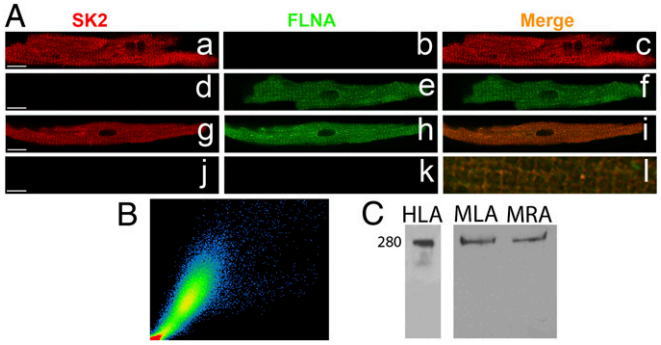

Fig. 2. FLNA is robustly expressed and colocalizes with SK2 in adult mouse atrial myocytes. (*A*, *a–f*) Immunofluorescence confocal microscopic imaging using single immunostaining with anti-SK2 (*a–c*) or anti-FLNA (*d–f*) antibodies. (*A*, *g–i*) Coimmunostaining using anti-SK2 and -FLNA antibodies. (*A*, *j* and k) Secondary antibody-only as negative controls. (*A*, *l*) Merged image from the coimmunostaining experiments showing colocalization of SK2 channel and FLNA proteins along the Z lines. (Scale bars, 10 μm.) (*B*) A scatter plot indicating a correlation coefficient between SK2 and FLNA of 0.80. All pixels in the images have been assigned a position on the scatter plot and are placed according to the intensity of red or green color. (*C*) Western blot analyses from human left atrium (HLA), mouse left atrium (MLA), and mouse right atrium (MRA).

mainly on the surface membrane (Fig. 4 *I–L*). In contrast, siRNA knockdown of FLNA showed a decrease in the surface membrane expression of SK2 channel (Fig. 4 *M–P*).

We further tested the localization of SK2 channel proteins after knockdown of FLNA using antibodies against various markers for the Golgi network, including anti-GM130, -Golgin84, and -P115 antibodies (Fig. S2*E*). In addition, anti-Rab5 (Fig. S2*E*) and anti-Rab8 antibodies (Fig. 4 *Q–U*) were used. The highest correlation coefficient with SK2 channel protein after knockdown of FLNA was observed by using anti-Rab8 antibody. Rab5 GTPase has been shown to be associated with early endosomes, whereas Rab8 GTPase is known to play a role in vesicular transport from the *trans*-Golgi network.

FLNA Augments Ca^{2+}-Activated K^+ Current in NMCMs and HEK 293 Cells. To further investigate the functional roles of FLNA on SK2 channel, whole-cell Ca^{2+}-activated K^+ current ($I_{K,Ca}$) was recorded from both NMCMs and HEK 293 cells (Fig. 5). Coexpression of SK2 channels with FLNA in HEK 293 cells yielded a significant increase in apamin-sensitive $I_{K,Ca}$ at −120 and +60 mV test potentials, respectively, compared with current recordings from cells expressing SK2 alone (Fig. 5 *A–C*). In NMCM, cells treated with FLNA siRNA showed a significant decrease in apamin-sensitive $I_{K,Ca}$ compared with cells treated with a nontargeting control siRNA (Fig. 5 *D–F*). Together, these recordings suggest that FLNA may promote the anterograde or inhibit the retrograde trafficking processes of SK2 channels.

SK2 Channel Trafficking Is Ca^{2+}- and CaM-Dependent. Previous studies have documented the critical role of CaM in SK2 channel trafficking (20). We hypothesize that an increase in $Ca^{2+}{}_i$,—for instance, as seen during rapid pacing or atrial arrhythmias—may promote the localization of SK2 channel on the membrane. The role of $Ca^{2+}{}_i$ on the membrane expression of SK2 channels was tested by using TIRF imaging and the same construct as in Fig. 3*A* in HEK 293 cells expressing SK2 with α-actinin2 (Fig. 6 *A*, *a–d*) and SK2 with FLNA (Fig. 6 *A*, *e–h*). Cells were treated with either vehicle alone (control; Fig. 6 *A*, *a*, *b*, *e*, and *f*) or 25 μM 1,2-Bis(2-aminophenoxy)ethane-*N*,*N*,*N*′,*N*′-tetraacetic acid tetraacetoxymethyl ester (BAPTA-AM) for 5 h (Fig. 6 *A*, *c*, *d*, *g*, and *h*). The fluorescence intensity on the membrane was significantly reduced when $Ca^{2+}{}_i$ was chelated by using BAPTA-AM in HEK 293 cells coexpressing SK2 and α-actinin2 (Fig. 6 *A*, *c* and *d* and *B*). In contrast, there were no significant changes in the membrane expression in HEK 293 cells expressing SK2 and FLNA treated with BAPTA-AM (Fig. 6 *A*, *g* and *h* and *B*).

As control experiments, a dominant-negative form of CaM (DN-CaM) was used and compared with wild-type CaM (Fig. 6*B*). The DN-CaM contains mutations at the four EF hand domains and is unable to bind Ca^{2+}. The fluorescence intensity on the membrane was significantly reduced in conditions in which cells were cotransfected with DN-CaM, confirming studies by Maylie et al. (20) suggesting an important role of CaM in the membrane trafficking of SK2 channel. We further tested the effects of endogenous CaM in promoting SK2 channel surface expression by comparing HEK 293 cells with or without coexpression with DN-CaM. There was a decrease in SK2 channel surface expression, but the findings were not statistically significant. Additionally, coexpression of SK2 channel with α-actinin2 resulted in a significant increase in the fluorescence intensity on the membrane compared with SK2 alone (Fig. 6*B*). This finding supported our prior study showing critical roles of α-actinin2 on the membrane localization of SK2 channels (14).

To test whether endogenous CaM alone suffices to confer Ca^{2+} sensitivities to the trafficking of SK2 channels, we performed experiments to test the effects of BAPTA-AM in cells expressing SK2 alone. No significant differences were detected in the cells expressing SK2 alone with or without pretreatment with BAPTA-AM (Fig. S3*A*). Similarly, to directly test whether α-actinin2 alone is sufficient to confer the Ca^{2+} sensitivities to the trafficking of SK2 channel, the effects of BAPTA-AM were tested in cells expressing SK2, α-actinin2, and DN-CaM. There were no significant differences between the two groups, suggesting that α-actinin2 alone does not suffice to confer the Ca^{2+} sensitivities to the trafficking of SK2 channel (Fig. S3*A*).

To further support the data obtained from TIRF imaging, we performed immunofluorescence confocal microscopy in HEK 293 cells cotransfected with human cardiac SK2 channel harboring extracellular hemagglutinin (HA) tag in the S1–S2 linker (SK2-HA) together with α-actinin2 or FLNA (Fig. 7 *A* and *B*, respectively). Cells were treated with either vehicle alone (control) or 25 μM BAPTA-AM (BAPTA) for 5 h. Cells were immunostained by using anti-HA antibody followed by chicken anti-mouse Alexa Fluor 488 secondary antibody with no permeabilization

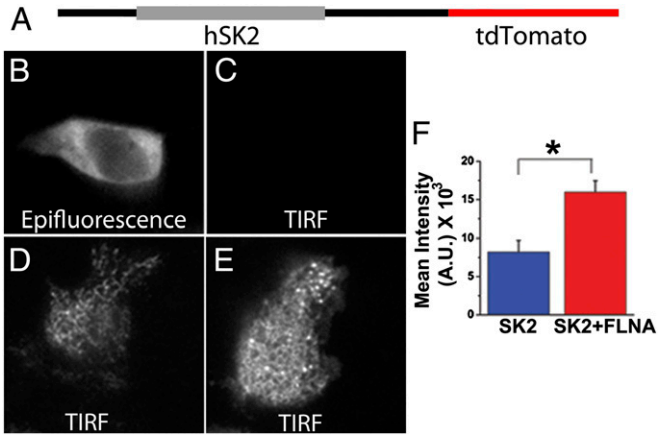

Fig. 3. FLNA enhances the membrane localization of SK2 channel proteins in HEK 293 cells. (*A*) Diagrammatic depiction of SK2–tdTomato construct used for TIRF-M. (*B* and *C*) Examples of TIRF microscopic images from a HEK 293 cell transfected with an empty vector containing only tdTomato showing fluorescence signals in epifluorescence mode, but not TIRF mode. (*D* and *E*) Examples of TIRF microscopic images from HEK 293 cells transfected with SK2–tdTomato alone (*D*) or with FLNA coexpression (*E*). (*F*) Summary data from TIRF-M showing a significant increase in fluorescence intensity in TIRF mode from HEK 293 cells coexpressing SK2–tdTomato and FLNA compared with SK2–tdTomato alone. A.U., arbitrary units. *$P < 0.05$ (n = 10–12 cells).

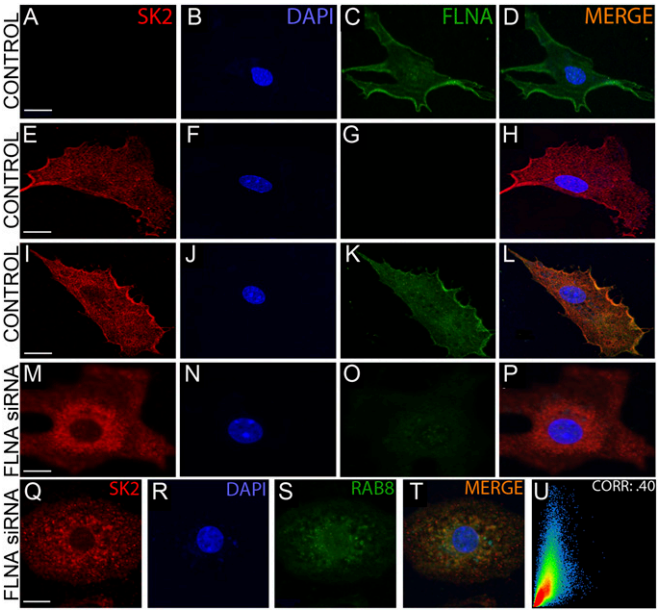

Fig. 4. siRNA knockdown of FLNA diminishes membrane localization of SK2 in NMCMs. (*A–L*) Photomicrographs of immunofluorescence confocal laser scanning microscopic images of NMCMs treated with a nontargeting siRNA (Control) stained with anti-FLNA (*A–D*) or anti-SK2 (*E–H*) antibodies or doubly immunostained with anti-SK2 and -FLNA antibodies (*I–L*) showing localization of SK2 channel protein on the plasma membrane. (*M–P*) NMCMs treated with FLNA siRNA doubly immunostained with anti-SK2 and -FLNA antibodies. The cells display a significant decrease in the membrane expression of SK2 channels. (*Q–T*) siRNA knockdown of FLNA protein results in the colocalization of SK2 channels with Rab8 GTPase. Cells were treated with anti-SK2 and -Rab8 antibodies. (*U*) Colocalization analysis shows a correlation coefficient of 0.40. (Scale bars, 10 μm.)

(NP). Cells were then permeabilized (P) and immunostained by using anti-HA antibody followed by rabbit anti-mouse Alexa Fluor 555 secondary antibody. Consistent with data in Fig. 6, there was a significant decrease in the fluorescence ratios (488/555) in HEK 293 cells coexpressing SK2 and α-actinin2 treated with BAPTA-AM compared with control (Fig. S3*B*; $^*P < 0.0004$). In contrast, no significant differences were observed in cells coexpressing SK2 and FLNA with or without BAPTA-AM (Fig. S3*B*). Control experiments were performed by using HEK 293 cells cotransfected with CaM compared with DN-CaM (Fig. S3*C*).

Computational Prediction of α-Actinin2 Bound to the C Terminus of SK2 Channels. Our previously published data demonstrate that the second EF hand of α-actinin2 protein interacts with the helical core region of the CaMBD in the C terminus of SK2 channel via hydrophobic interactions (14). Specifically, mutations of threonine (T431) and tryptophan (W432) residues—located within the helical core region of CaMBD of SK2 C terminus—to alanine disrupt the interaction. In contrast, mutations of threonine (T438) and leucine (L440) residues—located outside the helical core region—to alanine have no effects on the strength of the interactions. To understand the complex interactions between SK2 channels, α-actinin2, and CaM, as well as the Ca^{2+} dependence of SK2 channel trafficking, protein model visualization and analyses were performed by using the UCSF Chimera package (21). The final model for α-actinin2 bound to the CaMBD of SK2 channel was produced by a series of steps (Fig. S4). Fig. S4*A* shows the published crystal structure of the CaMBDs from two subunits of SK2 channel bound to two molecules of calcified CaM [Protein Data Bank (PDB) ID code 1G4Y] (22). Fig. S4*B* shows the published NMR structure of a molecule of apoCaM bound to $Na_v1.5$ (PDB ID code 2L53) (23). By using the matchmaker tool from the UCSF Chimera package, CaMBD of SK2 was superimposed onto $Na_v1.5$ (Fig. S4*C*). α-actinin2 was modeled after apoCaM by using the homology suite provided by Rosetta (Version 3.4; refs. 24 and 25) (Fig. S4*D*). This structure was then superimposed onto the crystal structure of SK2 and calcified CaM (1G4Y) to predict the binding of α-actinin2 within the helical core of the CaMBD of SK2 channel in the presence of calcified CaM (Fig. S4*E*).

Discussion

SK2 Channel Trafficking. The steady-state numbers of ion channel proteins on the plasma membrane are tightly and dynamically regulated. The channel proteins that are taken up via endocytosis assume multiple fates. They may be directed to lysosomal compartments or proteosomes for degradation or recycled via recycling or early endosomes. A number of interacting proteins, including cytoskeletal proteins and Rab GTPases, have been shown to direct the fate of channel proteins and vesicular transport (19, 26–28).

In our prior study, we demonstrated that α-actinin2, an F-actin–binding protein, interacts with the C terminus of SK2 channel, and the protein–protein interaction results in an increase in the membrane expression of SK2 channels (13, 14). In the present study, a multitude of approaches were used to demonstrate that FLNA, another actin-binding protein, interacts with the N terminus of SK2 channel to augment the surface membrane expression. Confocal microscopic imaging suggests that both SK2 and FLNA colocalize along the z lines in adult mouse cardiac myocytes. Similar to α-actinin2, siRNA-mediated knockdown of FLNA also reduces the SK2 channel membrane localization. However, in contrast to the knockdown of α-actinin2—which colocalizes SK2 channels with early endosomal markers, early endosomal antigen 1 (EEA1) and Rab5 GTPase (14)—knockdown of FLNA results in the colocalization of SK2 channels with Rab8 GTPase, a *trans*-Golgi marker. Functional studies using NMCMs show that siRNA knockdown of FLNA results in a decrease in $I_{K,Ca}$. In addition, coexpression of FLNA with SK2 channels in HEK 293 cells augments the density of SK2 channels on the membrane along with an increase in $I_{K,Ca}$, compared with the expression of SK2 alone.

Together, the results suggest that FLNA may up-regulate the surface membrane expression of SK2 channels by promoting forward trafficking from the *trans*-Golgi network. In contrast, we

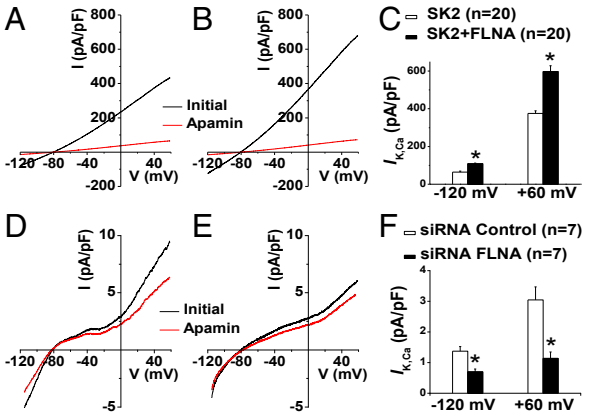

Fig. 5. FLNA modulates $I_{K,Ca}$ in both HEK 293 cells and NMCMs. (*A–C*) HEK 293 cells overexpressing SK2 alone (*A* and open bars in *C*) vs. cells coexpressing SK2 and FLNA (*B* and filled bars in *C*). After establishing the whole-cell mode, voltage-ramp protocols were applied from −120 to +60 mV from a holding potential of −55 mV using a slope of 0.36 mV/ms. Whole-cell currents were recorded before (black) and after (red) application of 100 pmol/L apamin. (*D–F*) NMCMs treated with control siRNA (*D* and open bars in *F*) or FLNA siRNA (*E* and filled bars in *F*). (*C* and *F*) Summary data of apamin-sensitive $I_{K,Ca}$ at −120 and +60 mV from HEK 293 cells (*C*; $n = 20$ cells) and NMCMs (*F*; $n = 7$ cells). $^*P < 0.05$.

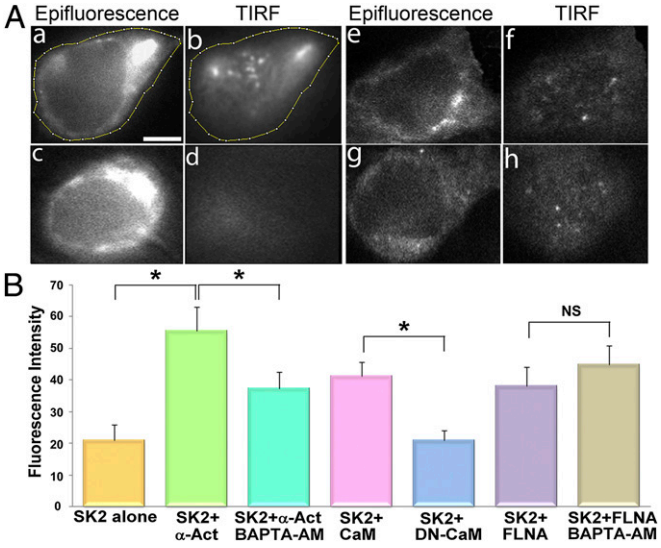

Fig. 6. SK2 channel trafficking is Ca^{2+}- and CaM-dependent. (*A*) Examples of TIRF microscopic imaging in epifluorescence (*a*, *c*, *e*, and *g*) and TIRF (*b*, *d*, *f*, and *h*) modes from HEK 293 cells expressing SK2 with α-actinin2 (*a*–*d*) and SK2 with FLNA (*e*–*h*). Live-cell imaging was obtained from cells in normal culture medium (*a*, *b*, *e*, and *f*) compared with cells pretreated with 25 μM BAPTA-AM for 5 h (*c*, *d*, *g*, and *h*). (Scale bar, 5 μm.) (*B*) Summary data of fluorescence intensity in the TIRF mode showing a significant decrease in the fluorescence intensity in cells expressing SK2 and α-actinin2 after pretreatment with BAPTA-AM. *$P < 0.05$ ($n = 8$–10 cells per group). There were no significant differences in the fluorescence intensity in cells expressing SK2 and FLNA in control culture medium or after pretreatment with BAPTA-AM. As control experiments, DN-CaM was used and compared with wild-type CaM. The fluorescence intensity on the membrane was significantly reduced in conditions where cells were cotransfected with DN-CaM. *$P < 0.05$ ($n = 8$–10 cells per group). NS, not significant.

have previously shown that knockdown of α-actinin2 results in the localization of SK2 channels within early endosomes (EEA1 and Rab5 GTPase), suggesting that α-actinin2 may promote forward trafficking via enhancing the recycling from early endosomes or decreasing the retrograde trafficking pathway (14). Further experiments are required to pinpoint additional trafficking pathway(s) involved. Finally, using live-cell and immunofluorescence imaging, we demonstrate that $Ca^{2+}{}_i$ plays a critical role in the membrane localization of SK2 channel when the channel is coexpressed with α-actinin2. Indeed, an increase in $Ca^{2+}{}_i$—for instance, during rapid AF or atrial tachycardia—is predicted to result in an increase in SK2 channel expression, leading to shortening of the action potential.

Role of SK Channels in the Heart. We have previously identified different isoforms of SK channels [SK1 ($K_{Ca}2.1$), SK2 ($K_{Ca}2.2$), and SK3 ($K_{Ca}2.3$)] in the heart (6, 7). The channels are found to be expressed at a higher level in atria compared with ventricles (6). Our findings have subsequently been supported by several different laboratories (9, 29–33). We further demonstrate that SK channels play critical roles in pacemaking cells (34). The SK2 knockout mice have been shown to be prone to inducible AF (8). Conversely, a recent study by Diness et al. suggests that inhibition of $I_{K,Ca}$ may prevent AF (9). These findings emphasize the critical impact of the precise control of dynamic SK channel expression on the surface membrane for the maintenance of normal action potentials in atria. Overall, there is growing evidence supporting the significant role of SK channels in cardiac excitability.

FLNA as an Interacting Partner. Ion-channel trafficking is a dynamic and complex process, which depends on a number of interacting proteins (27, 28). The importance of interacting partners is exemplified by mutations in ankyrin B leading to long QT syndrome, sinus node dysfunction, and atrial fibrillation (11, 12). The role of FLNA as a structural protein has long been established. However, only recently has FLNA been identified as an interacting partner of membrane proteins, including K^+ channels. FLNA interaction with $K_v4.2$ in neurons and Kir2.1 in smooth muscle cells localizes the channels to certain hotspots on the plasma membrane (17, 18). Interactions with large-conductance Ca^{2+}-activated K^+ (BK) channels also increase the membrane expression (35). In addition, FLNA has been implicated in the trafficking of cystic fibrosis transmembrane conductance regulator and a chemokine receptor, CCR2B (15, 19). FLNA is modulated by adapter proteins and phosphorylated at multiple sites by several kinases (36, 37). These mechanisms can potentially regulate FLNA binding partners and lead to downstream consequences, including SK2 localization and membrane excitation.

SK2 Channel Trafficking is Ca^{2+}- and CaM-Dependent. Previous data suggest that the membrane trafficking of SK2 channels is CaM-dependent (20). In addition, burst pacing has been shown to induce SK2 channel trafficking to the membrane in pulmonary veins of rabbit atria (29). We hypothesize that SK2 channel trafficking may be Ca^{2+}-dependent. Indeed, our data using TIRF imaging and immunofluorescence staining demonstrate that the membrane localization of SK2 channels is sensitive to changes in $Ca^{2+}{}_i$ only when the channels are coexpressed with α-actinin2, but not FLNA.

Molecular modeling was performed to understand the Ca^{2+} dependence of SK2 channel trafficking. The complex interactions between SK2 channels and α-actinin2 in the presence of calcified CaM were further tested by using protein model visualization and analyses. We took advantage of a previous crystal structure of the CaMBD of SK2 channel with Ca^{2+}/CaM complex, which demonstrates that Ca^{2+} binds to the EF hands in the N lobe of CaM. Once CaM becomes calcified, it interacts with the CaMBD from two different subunits of SK2 channel by interacting with three α-helices—two from one CaMBD subunit and one from the other (PDB ID code 1G4Y) (22). Using computational modeling and the previous crystal structure of CaMBD of SK2 channel (22) together with our published study of α-actinin2 interaction with CaMBD (14), we predict the binding of α-actinin2 within the helical core of the CaMBD of SK2 channel in the

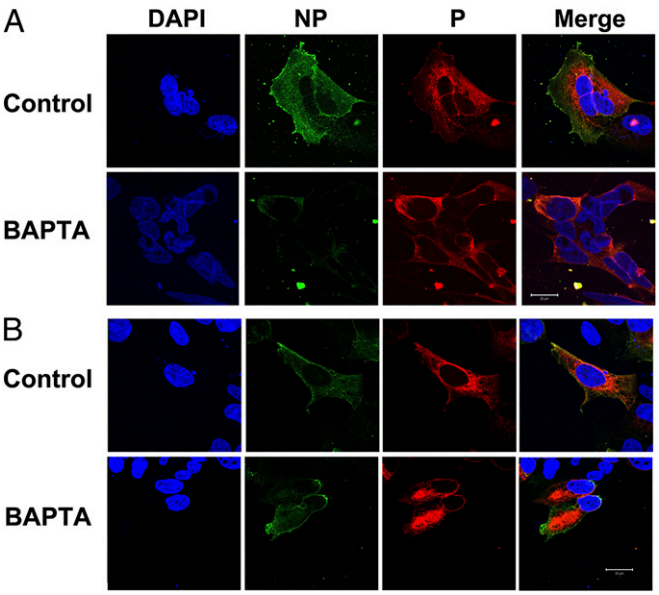

Fig. 7. Immunofluorescence confocal microscopy of HEK 293 cells. HEK 293 cells were cotransfected with human cardiac SK2–HA together with α-actinin (*A*) or FLNA (*B*). Cells were treated with either vehicle alone (control) or 25 μM BAPTA-AM (BAPTA) for 5 h. (Scale bars, 20 μm.)

presence of calcified CaM. The binding of α-actinin2 to SK2 channel maybe enhanced when CaM is calcified by recruiting the additional SK2 subunit, leading to an increase in the membrane expression of SK2 channels. Consistent with this notion, our data suggest that either CaM or α-actinin2 alone does not suffice to confer the Ca^{2+} sensitivities to the trafficking of SK2 channels.

Future Directions. Our findings suggest that the Ca^{2+}-dependent trafficking of SK2 channel depends on the interaction between the C-terminal domain of the channels with CaM and α-actinin2, but not FLNA. Several possibilities exist to explain the findings. It is conceivable that FLNA-bound SK2 channel may not be able to interact with CaM. Alternatively, there may be distinct pools of SK2 channels interacting with α-actinin2 or FLNA. These different hypotheses will need to be tested in additional studies.

We have previously shown that $I_{K,Ca}$ predominates in the atria compared with the ventricles and that SK2 knockout mice exhibit inducible AF (6–8). In addition to our previous studies showing the role of α-actinin2 in trafficking of SK2 channels (13, 14), we have now identified the role of FLNA in modifying the number of channels on the plasma membrane. Further studies deciphering specific trafficking pathways of SK2 channels may lead to on-target therapies modulating $I_{K,Ca}$ in AF. Finally, our data suggest that an increase in $Ca^{2+}{}_i$, as is evident during rapid AF or atrial tachycardia, is predicted to result in an increase in SK2 channel expression, leading to shortening of the atrial action potentials and maintenance of the arrhythmias.

Materials and Methods

Detailed methods are presented in *SI Materials and Methods*.

Yeast Two-Hybrid Screenings. Yeast two-hybrid screenings were performed as described (13).

Immunofluorescence Confocal Laser Scanning Microscopy. Immunofluorescence confocal microscopy was performed as described (13, 14).

Western Blot Analysis. Human heart tissues were procured from a commercial source (T-Cubed). Western blot analyses were performed as described (13, 14).

$I_{K,Ca}$ Recordings. Whole-cell $I_{K,Ca}$ was recorded from isolated NMCMs and transfected HEK 293 cells (ATCC) by using patch-clamp techniques (6, 38).

TIRF-M. Human cardiac SK2 channel fused with tdTomato fluorescent protein and expressed in HEK 293 cells was used for TIRF-M.

ACKNOWLEDGMENTS. Special thanks to Dr. P. M. Ghosh (University of California, Davis), Dr. D. Fedida (University of British Columbia), and Dr. J. H. Hartwig (Harvard Medical School) for human FLNA in pREP4 vector, α-actinin2 cDNA in pcDNA3 vector, and the M2 cell line, respectively. This work was supported by National Institutes of Health/National Heart, Lung, and Blood Institute Grants R01 HL085727 and R01 HL085844 (to N.C.); R01 HL077281 and HL079071 (to A.A.K.); and National Institute on Deafness and Other Communication Disorders Grants R01 DC003826, R01 DC007592, and R01 DC010386 (to E.N.Y.), and Veterans Affairs Merit Review Grant I01 BX000576 (to N.C.).

1. Köhler M, et al. (1996) Small-conductance, calcium-activated potassium channels from mammalian brain. *Science* 273(5282):1709–1714.
2. Vergara C, Latorre R, Marrion NV, Adelman JP (1998) Calcium-activated potassium channels. *Curr Opin Neurobiol* 8(3):321–329.
3. Stocker M (2004) Ca^{2+}-activated K^+ channels: Molecular determinants and function of the SK family. *Nat Rev Neurosci* 5(10):758–770.
4. Pennefather P, Lancaster B, Adams PR, Nicoll RA (1985) Two distinct Ca-dependent K currents in bullfrog sympathetic ganglion cells. *Proc Natl Acad Sci USA* 82(9): 3040–3044.
5. Pedarzani P, et al. (2005) Specific enhancement of SK channel activity selectively potentiates the afterhyperpolarizing current $I_{(AHP)}$ and modulates the firing properties of hippocampal pyramidal neurons. *J Biol Chem* 280(50):41404–41411.
6. Xu Y, et al. (2003) Molecular identification and functional roles of a $Ca^{(2+)}$-activated K^+ channel in human and mouse hearts. *J Biol Chem* 278(49):49085–49094.
7. Tuteja D, et al. (2005) Differential expression of small-conductance Ca^{2+}-activated K^+ channels SK1, SK2, and SK3 in mouse atrial and ventricular myocytes. *Am J Physiol Heart Circ Physiol* 289(6):H2714–H2723.
8. Li N, et al. (2009) Ablation of a Ca^{2+}-activated K^+ channel (SK2 channel) results in action potential prolongation in atrial myocytes and atrial fibrillation. *J Physiol* 587(Pt 5): 1087–1100.
9. Diness JG, et al. (2010) Inhibition of small-conductance Ca^{2+}-activated K^+ channels terminates and protects against atrial fibrillation. *Circ Arrhythm Electrophysiol* 3(4): 380–390.
10. Schumacher SM, Martens JR (2010) Ion channel trafficking: A new therapeutic horizon for atrial fibrillation. *Heart Rhythm* 7(9):1309–1315.
11. Chauhan VS, Tuvia S, Buhusi M, Bennett V, Grant AO (2000) Abnormal cardiac $Na^{(+)}$ channel properties and QT heart rate adaptation in neonatal ankyrin(B) knockout mice. *Circ Res* 86(4):441–447.
12. Le Scouarnec S, et al. (2008) Dysfunction in ankyrin-B-dependent ion channel and transporter targeting causes human sinus node disease. *Proc Natl Acad Sci USA* 105(40):15617–15622.
13. Lu L, et al. (2007) Molecular coupling of a Ca^{2+}-activated K^+ channel to L-type Ca^{2+} channels via alpha-actinin2. *Circ Res* 100(1):112–120.
14. Lu L, et al. (2009) Alpha-actinin2 cytoskeletal protein is required for the functional membrane localization of a Ca^{2+}-activated K^+ channel (SK2 channel). *Proc Natl Acad Sci USA* 106(43):18402–18407.
15. Minsaas L, et al. (2010) Filamin A binds to CCR2B and regulates its internalization. *PLoS ONE* 5(8):e12212.
16. Gravante B, et al. (2004) Interaction of the pacemaker channel HCN1 with filamin A. *J Biol Chem* 279(42):43847–43853.
17. Petrecca K, Miller DM, Shrier A (2000) Localization and enhanced current density of the $K_v4.2$ potassium channel by interaction with the actin-binding protein filamin. *J Neurosci* 20(23):8736–8744.
18. Sampson LJ, Leyland ML, Dart C (2003) Direct interaction between the actin-binding protein filamin-A and the inwardly rectifying potassium channel, Kir2.1. *J Biol Chem* 278(43):41988–41997.
19. Thelin WR, et al. (2007) Direct interaction with filamins modulates the stability and plasma membrane expression of CFTR. *J Clin Invest* 117(2):364–374.
20. Maylie J, Bond CT, Herson PS, Lee W-S, Adelman JP (2004) Small conductance Ca^{2+}-activated K^+ channels and calmodulin. *J Physiol* 554(Pt 2):255–261.
21. Pettersen EF, et al. (2004) UCSF Chimera—a visualization system for exploratory research and analysis. *J Comput Chem* 25(13):1605–1612.
22. Schumacher MA, Rivard AF, Bächinger HP, Adelman JP (2001) Structure of the gating domain of a Ca^{2+}-activated K^+ channel complexed with Ca^{2+}/calmodulin. *Nature* 410(6832):1120–1124.
23. Chagot B, Chazin WJ (2011) Solution NMR structure of apo-calmodulin in complex with the IQ motif of human cardiac sodium channel $Na_v1.5$. *J Mol Biol* 406(1):106–119.
24. Raman S, et al. (2009) Structure prediction for CASP8 with all-atom refinement using Rosetta. *Proteins* 77(Suppl 9):89–99.
25. Chivian D, Baker D (2006) Homology modeling using parametric alignment ensemble generation with consensus and energy-based model selection. *Nucleic Acids Res* 34(17):e112.
26. Stenmark H (2009) Rab GTPases as coordinators of vesicle traffic. *Nat Rev Mol Cell Biol* 10(8):513–525.
27. Zhang SS, Shaw RM (2013) Multilayered regulation of cardiac ion channels. *Biochim Biophys Acta* 1833(4):876–885.
28. Calaghan SC, Le Guennec JY, White E (2004) Cytoskeletal modulation of electrical and mechanical activity in cardiac myocytes. *Prog Biophys Mol Biol* 84(1):29–59.
29. Ozgen N, et al. (2007) Early electrical remodeling in rabbit pulmonary vein results from trafficking of intracellular SK2 channels to membrane sites. *Cardiovasc Res* 75(4): 758–769.
30. Diness JG, et al. (2011) Effects on atrial fibrillation in aged hypertensive rats by Ca^{2+}-activated K^+ channel inhibition. *Hypertension* 57(6):1129–1135.
31. Skibsbye L, Diness JG, Sørensen US, Hansen RS, Grunnet M (2011) The duration of pacing-induced atrial fibrillation is reduced in vivo by inhibition of small conductance $Ca^{(2+)}$-activated $K^{(+)}$ channels. *J Cardiovasc Pharmacol* 57(6):672–681.
32. Chua SK, et al. (2011) Small-conductance calcium-activated potassium channel and recurrent ventricular fibrillation in failing rabbit ventricles. *Circ Res* 108(8): 971–979.
33. Chang PC, et al. (2013) Heterogeneous upregulation of apamin-sensitive potassium currents in failing human ventricles. *J Am Heart Assoc* 2(1):e004713.
34. Zhang Q, et al. (2008) Functional roles of a Ca^{2+}-activated K^+ channel in atrioventricular nodes. *Circ Res* 102(4):465–471.
35. Kim EY, Ridgway LD, Dryer SE (2007) Interactions with filamin A stimulate surface expression of large-conductance Ca^{2+}-activated K^+ channels in the absence of direct actin binding. *Mol Pharmacol* 72(3):622–630.
36. O'Connell MP, et al. (2009) Wnt5A activates the calpain-mediated cleavage of filamin A. *J Invest Dermatol* 129(7):1782–1789.
37. Ohta Y, Hartwig JH, Stossel TP (2006) FilGAP, a Rho- and ROCK-regulated GAP for Rac binds filamin A to control actin remodelling. *Nat Cell Biol* 8(8):803–814.
38. Hamill OP, Marty A, Neher E, Sakmann B, Sigworth FJ (1981) Improved patch-clamp techniques for high-resolution current recording from cells and cell-free membrane patches. *Pflugers Arch* 391(2):85–100.